Supporting Information

Bioinspired Strategy for Controlled Polymerization and Photopatterning of Plant Polyphenols

Farid Behboodi-Sadabad,[†,‡] Huijie Zhang,[§] Vanessa Trouillet,[⊥,∥] Alexander Welle,[∥,#] Nicolas Plumeré,[§] Pavel A. Levkin*[,†,‡]

[†]Institute of Organic Chemistry, Karlsruhe Institute of Technology, 76021 Karlsruhe, Germany

[‡]Institute of Toxicology and Genetics, Karlsruhe Institute of Technology, 76344 Eggenstein-Leopoldshafen, Germany

[§]Center for Electrochemical Sciences, Ruhr-Universität Bochum, D-44780 Bochum, Germany

[⊥]Institute for Applied Materials, Karlsruhe Institute of Technology, 76344 Eggenstein-Leopoldshafen, Germany

[∥]Karlsruhe Nano Micro Facility, Karlsruhe Institute of Technology, 76344 Eggenstein-Leopoldshafen, Germany

[#]Institute of Functional Interfaces, Karlsruhe Institute of Technology, 76344 Eggenstein-Leopoldshafen, Germany

*E-mail: levkin@kit.edu

Scheme S1. Oxidation products of sodium ascorbate (SA), uric acid (UA), and glutathione (GSH) in the presence of oxygen and radical derivatives of oxygen (ROS).[1]

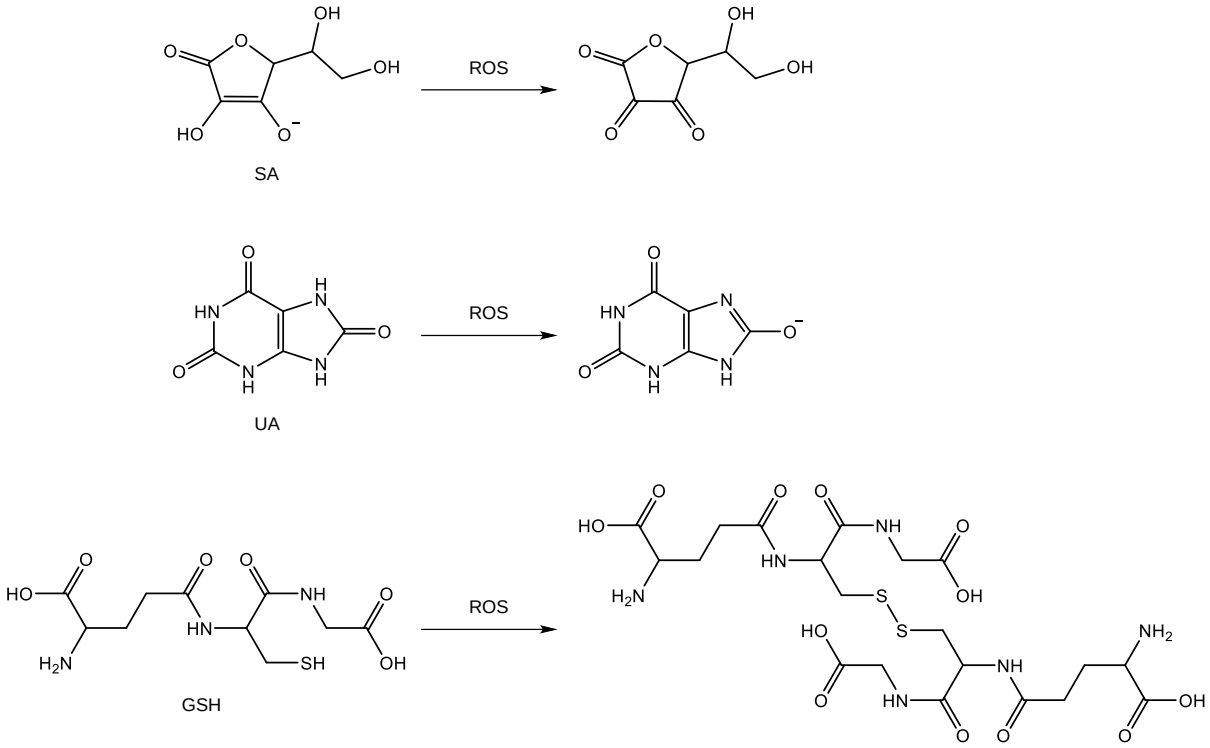

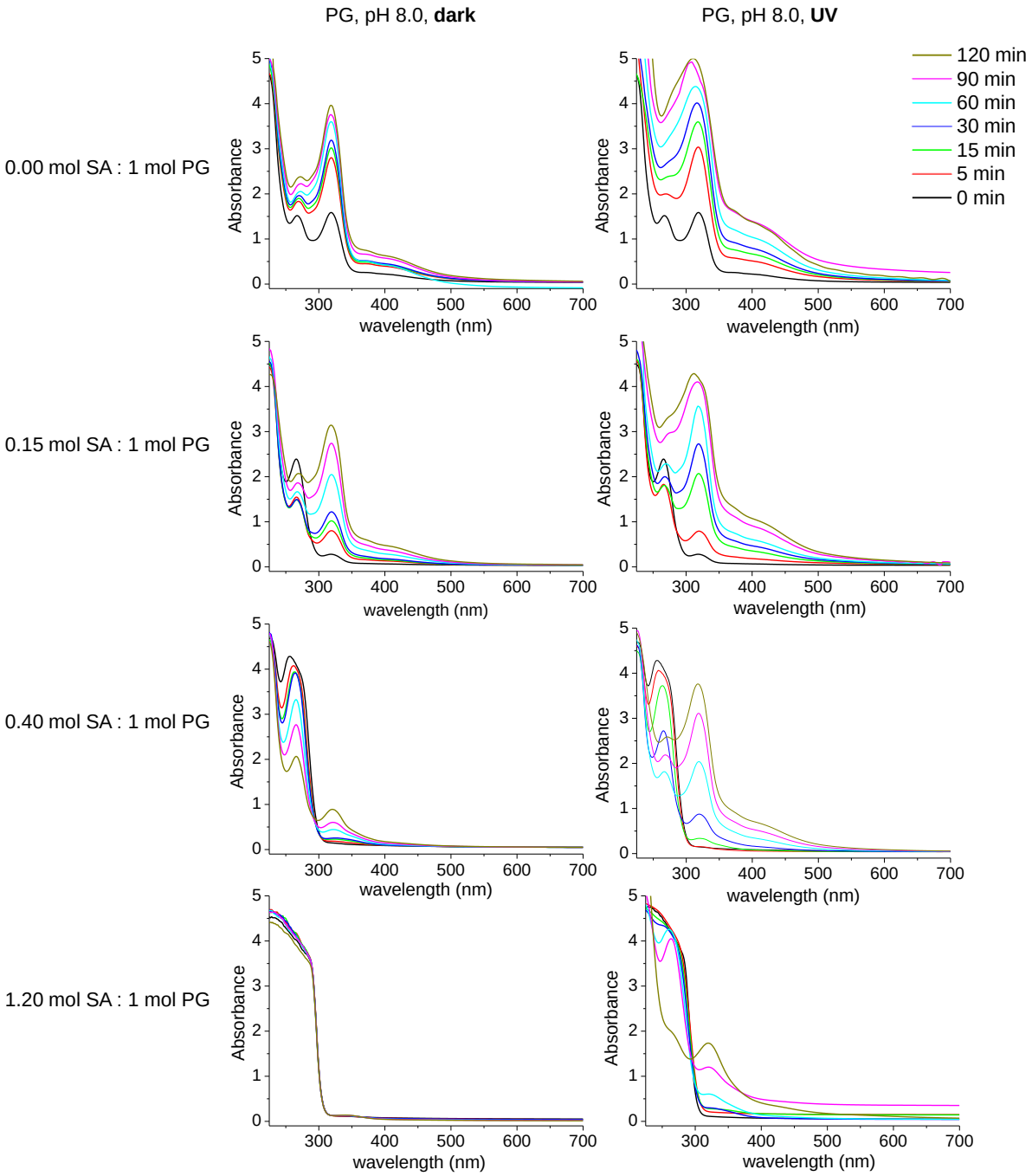

Figure S1. UV-vis spectra of PG solution (0.2 mg/mL) at phosphate buffer 5 mmol/L at pH 8.0, stored in dark environment (left) and after UV irradiation (right) containing SA measured at different time intervals.

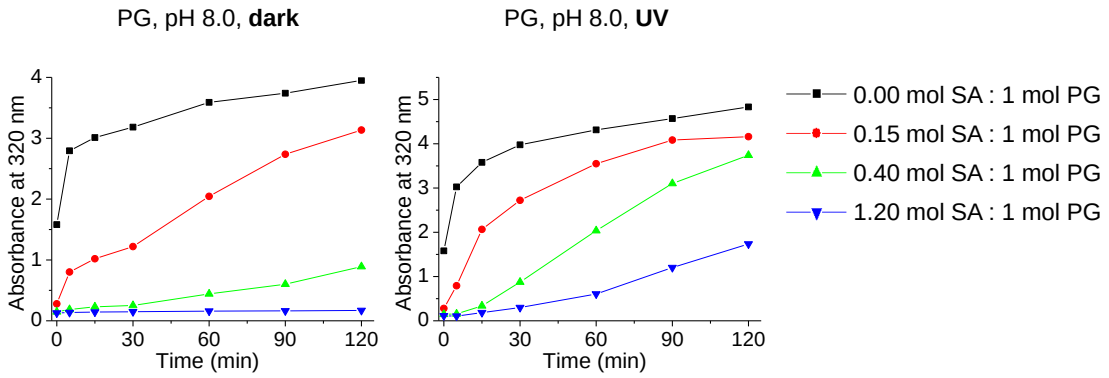

Figure S2. Effect of natural antioxidants on PG polymerization with and without UV irradiation. The graphs show UV absorbance of PG solutions (0.2 mg/mL, phosphate buffer 5 mmol/L, pH 8.0) at 320 nm. PG polymerization solution in the dark (left) and under UV irradiation (right) in the presence of SA (with different molar ratios of antioxidants to PG).

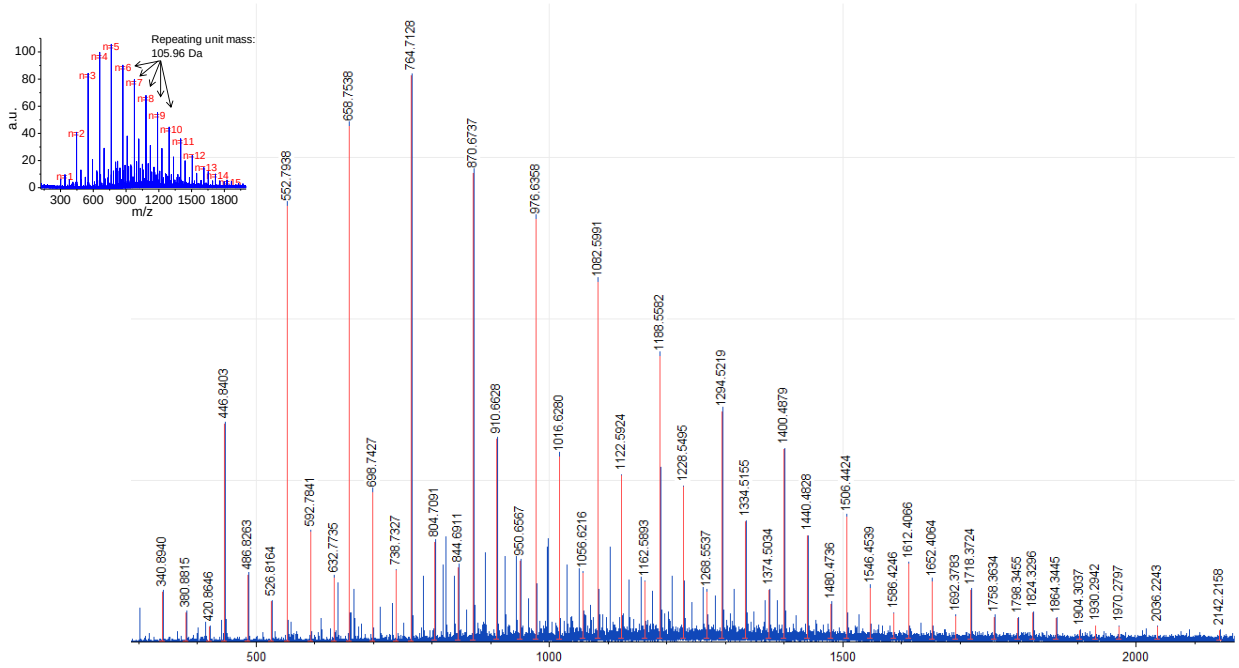

Figure S3. ESI-MS spectra (positive mode) of the PG solution (0.2 mg/mL of PG in phosphate buffer, 5 mmol/L, pH 8.0; 1.2:1, SA:PG molar ratio) after UV irradiation for 2h with labeled peaks. There are three sequential mass series which are easily distinguishable in the mass spectrum. The mass difference between first (with the highest intensity) and second series, and also mass difference between second and third series is 39.99 m/z. Other mass series with low intensities in the spectrum can be observed.

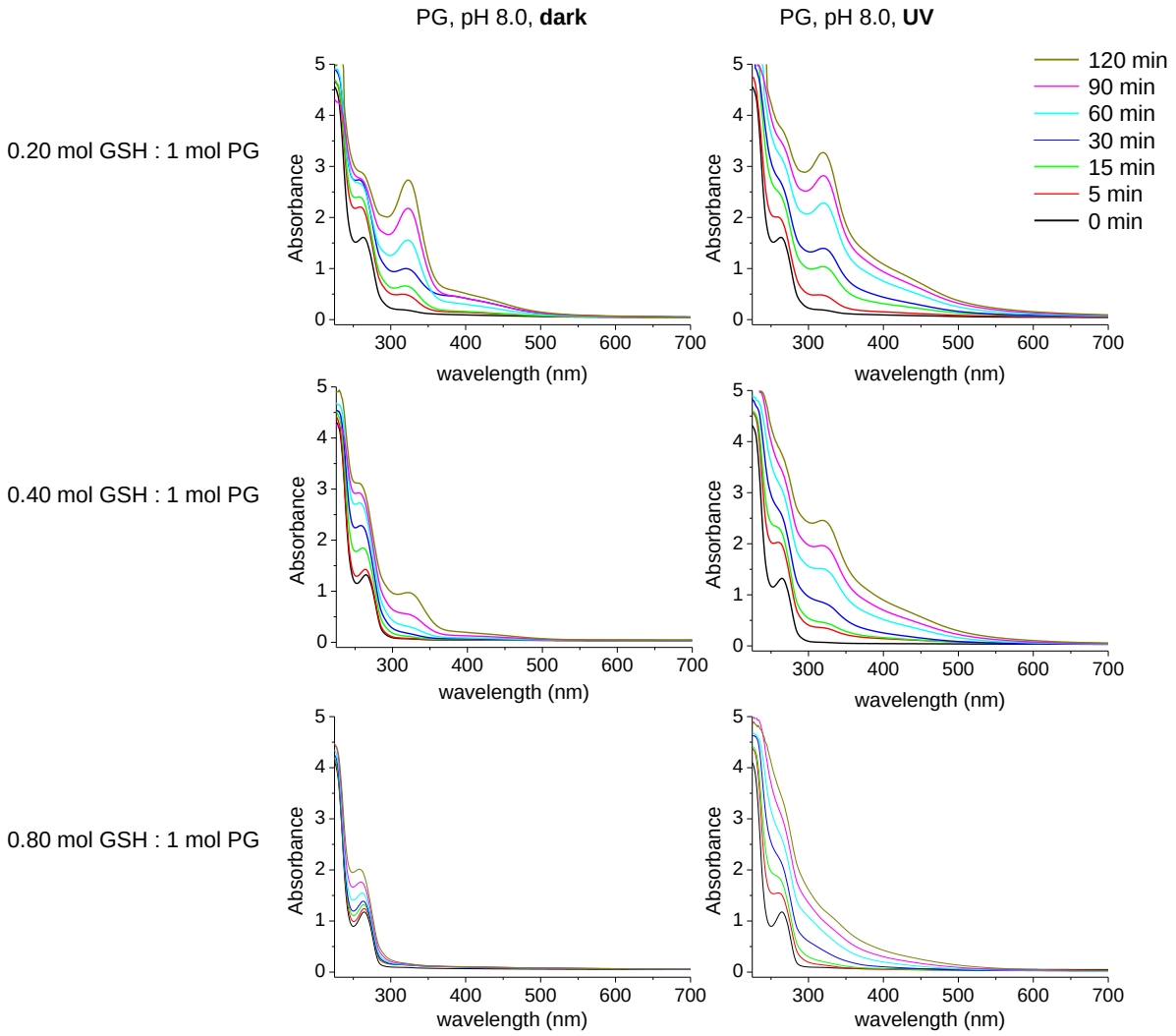

Figure S4. UV-vis spectra of PG solution (0.2 mg/mL) at phosphate buffer 5 mmol/L at pH 8.0, stored in dark environment (left) and after UV irradiation (right) containing GSH measured at different time intervals.

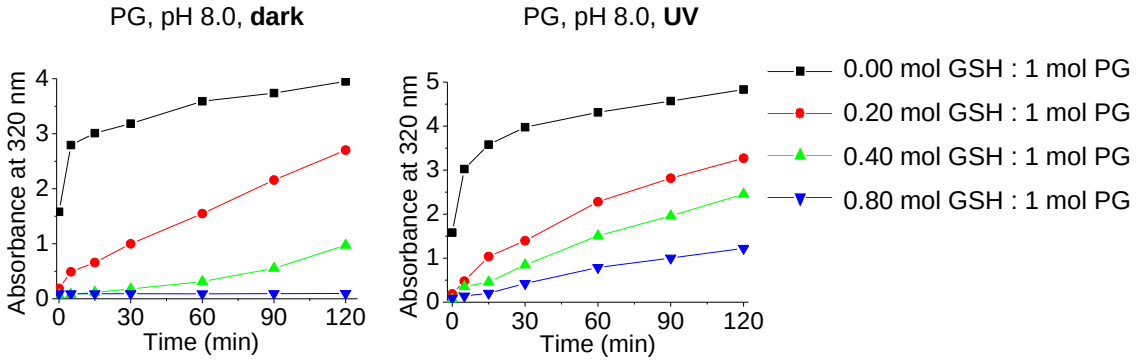

Figure S5. Effect of natural antioxidants on PG polymerization with and without UV irradiation. The graphs show UV absorbance of PG solutions (0.2 mg/mL, phosphate buffer 5 mmol/L, pH 8.0) at 320 nm. PG polymerization solution in the dark (left) and under UV irradiation (right) in the presence of GSH (with different molar ratios of antioxidants to PG).

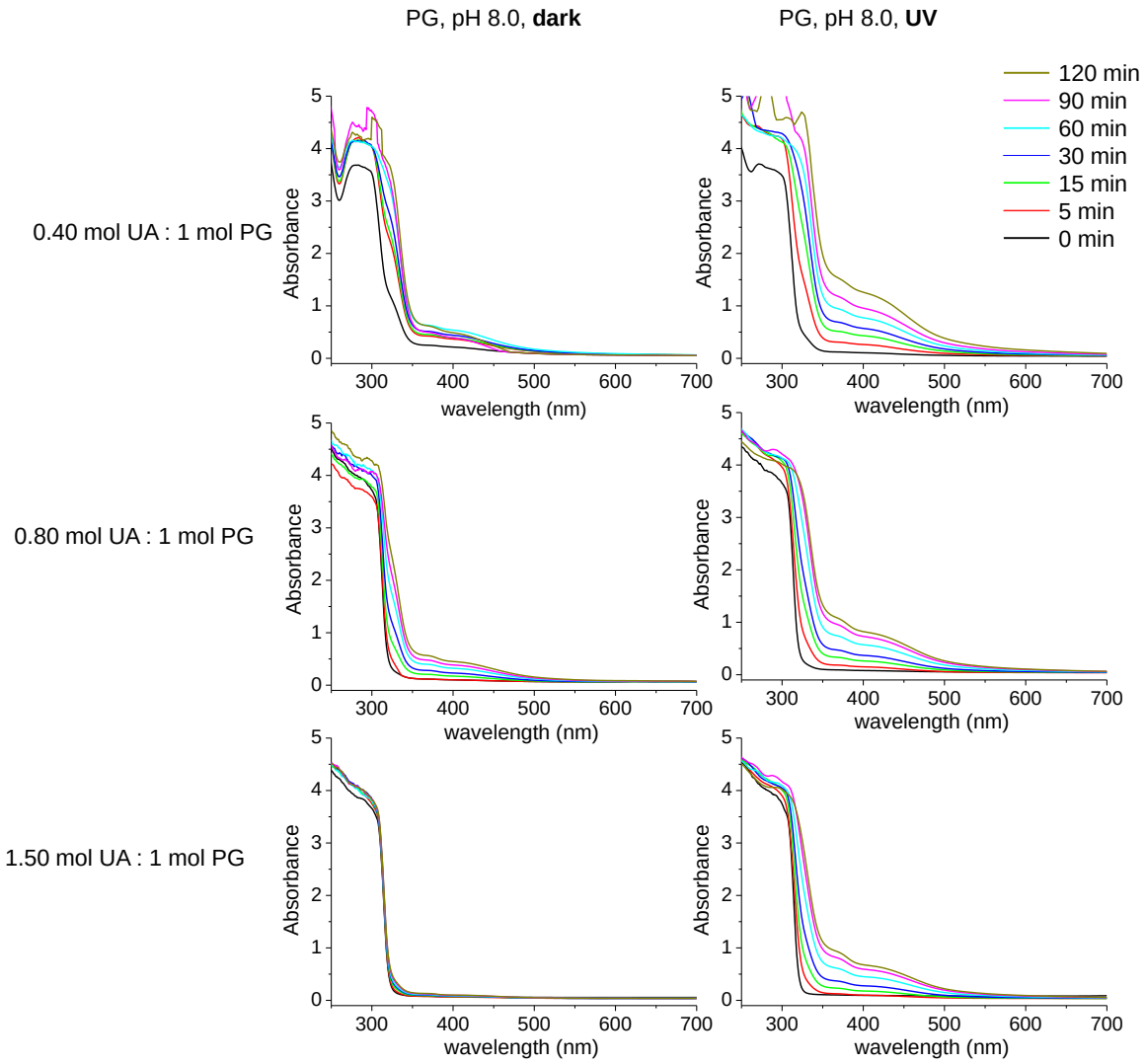

Figure S6. UV-vis spectra of PG solution (0.2 mg/mL) at phosphate buffer 5 mmol/L at pH 8.0, stored in dark environment (left) and after UV irradiation (right) containing UA measured at different time intervals.

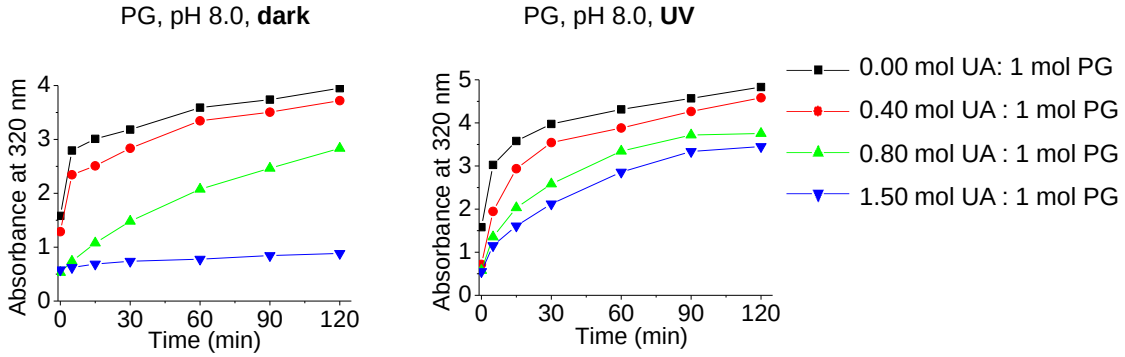

Figure S7. Effect of natural antioxidants on PG polymerization with and without UV irradiation. The graphs show UV absorbance of PG solutions (0.2 mg/mL, phosphate buffer 5 mmol/L, pH 8.0) at 320 nm. PG polymerization solution in the dark (left) and under UV irradiation (right) in the presence of UA (with different molar ratios of antioxidants to PG).

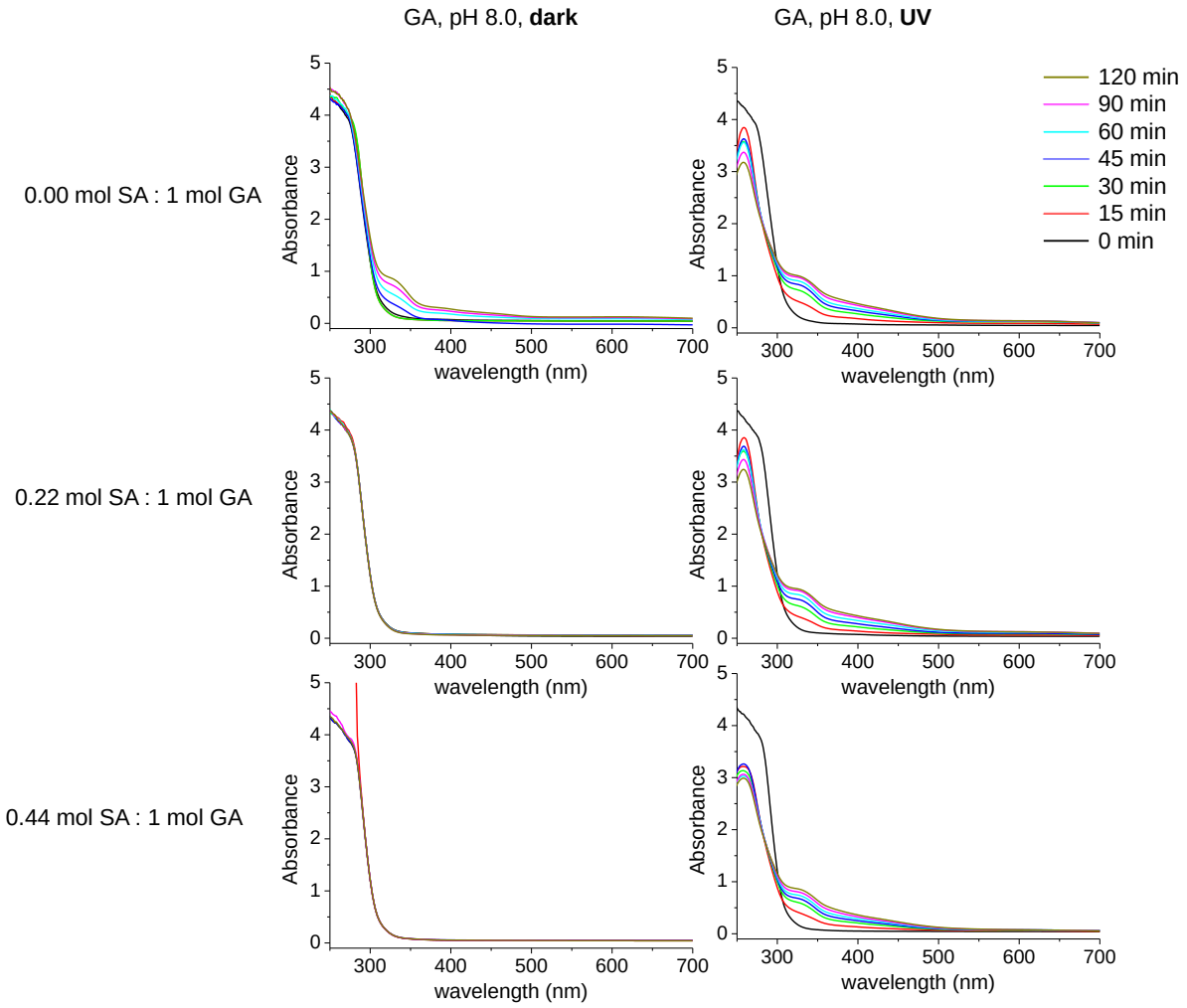

Figure S8. UV-vis spectra of GA solution (0.2 mg/mL) at phosphate buffer 5 mmol/L at pH 8.0, stored in dark environment (left) and after UV irradiation (right) containing SA measured at different time intervals.

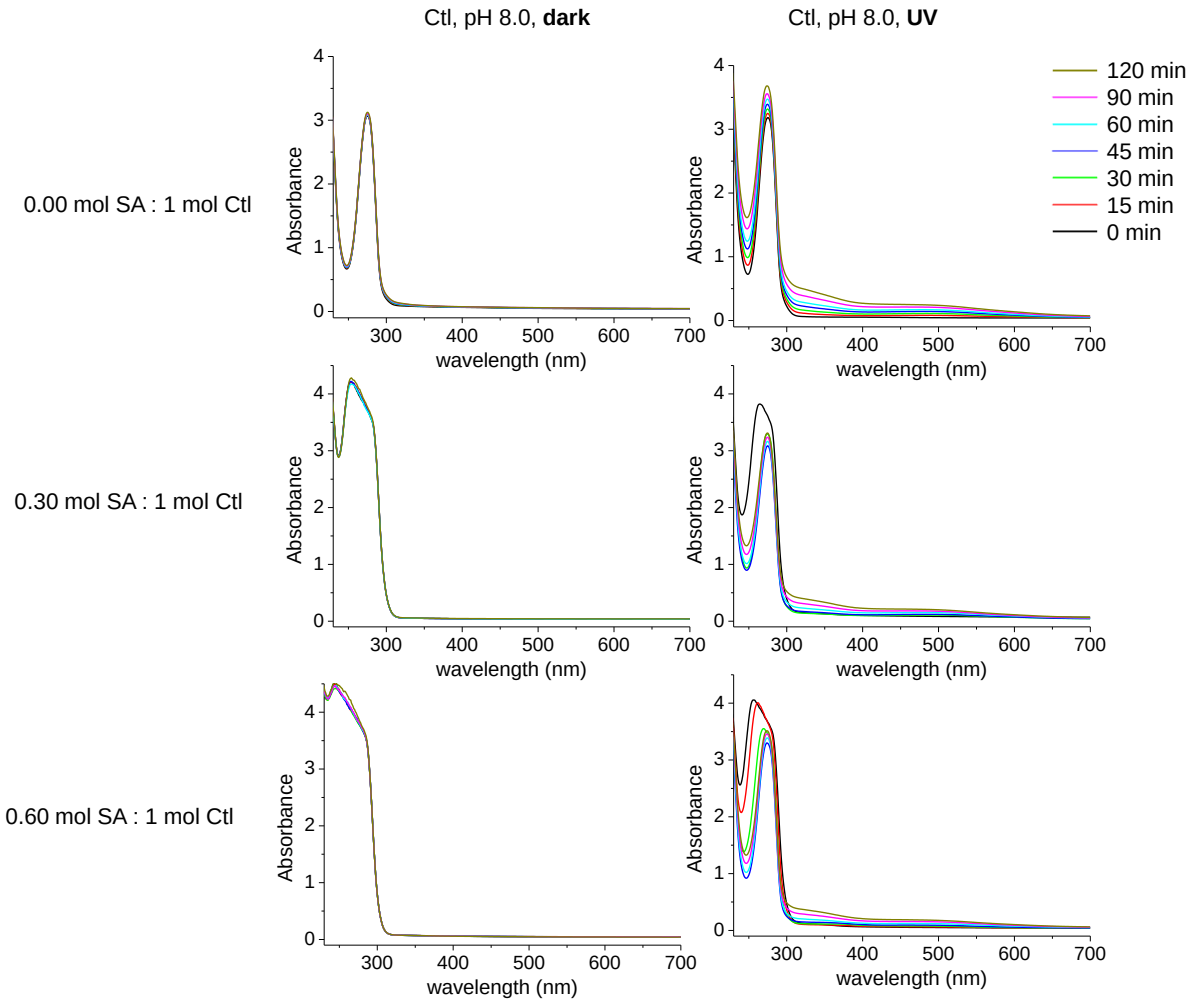

Figure S9. UV-vis spectra of Ctl solution (0.2 mg/mL) at phosphate buffer 5 mmol/L at pH 8.0, stored in dark environment (left) and after UV irradiation (right) containing SA measured at different time intervals.

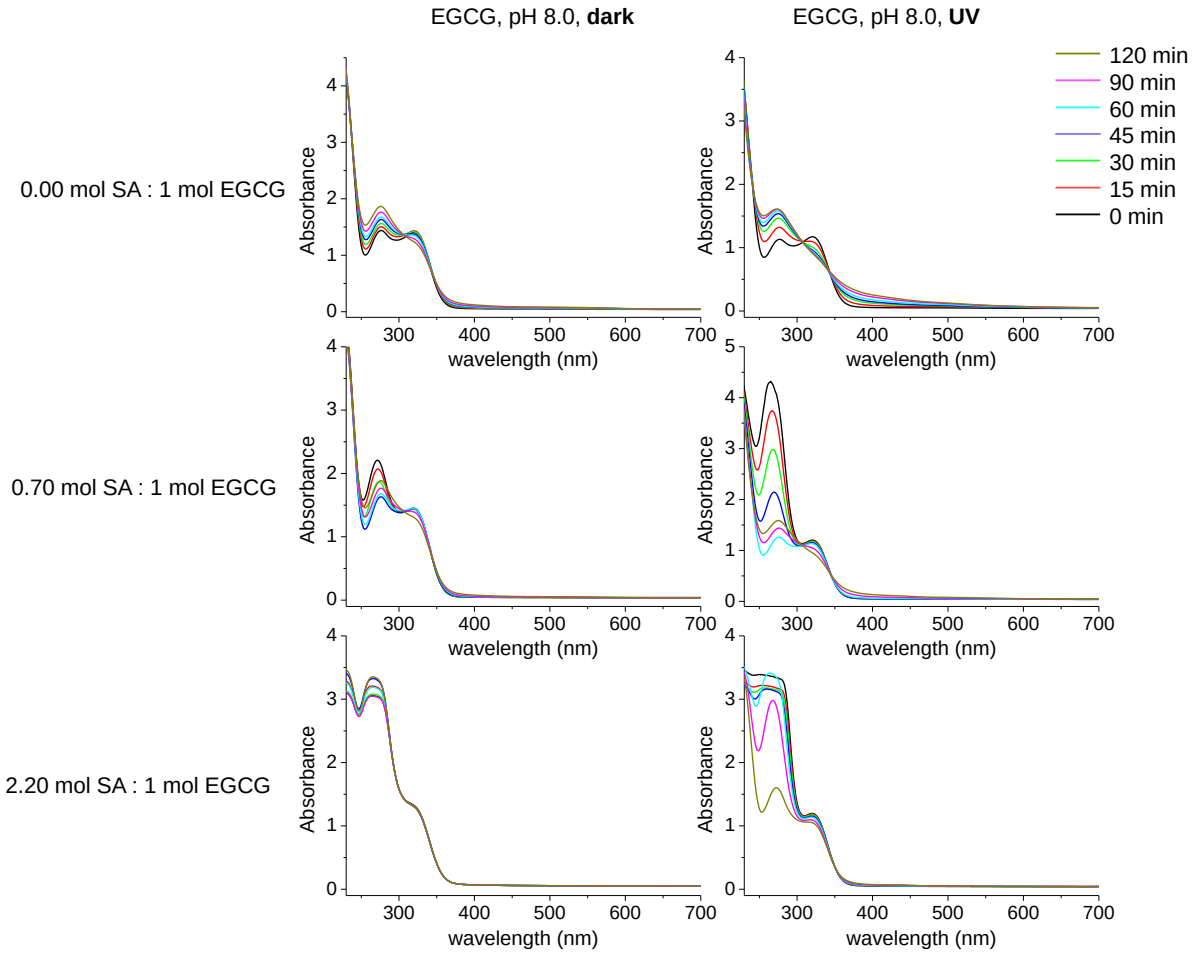

Figure S10. UV-vis spectra of EGCG solution (0.2 mg/mL) at phosphate buffer 5 mmol/L at pH 8.0, stored in dark environment (left) and after UV irradiation (right) containing SA measured at different time intervals.

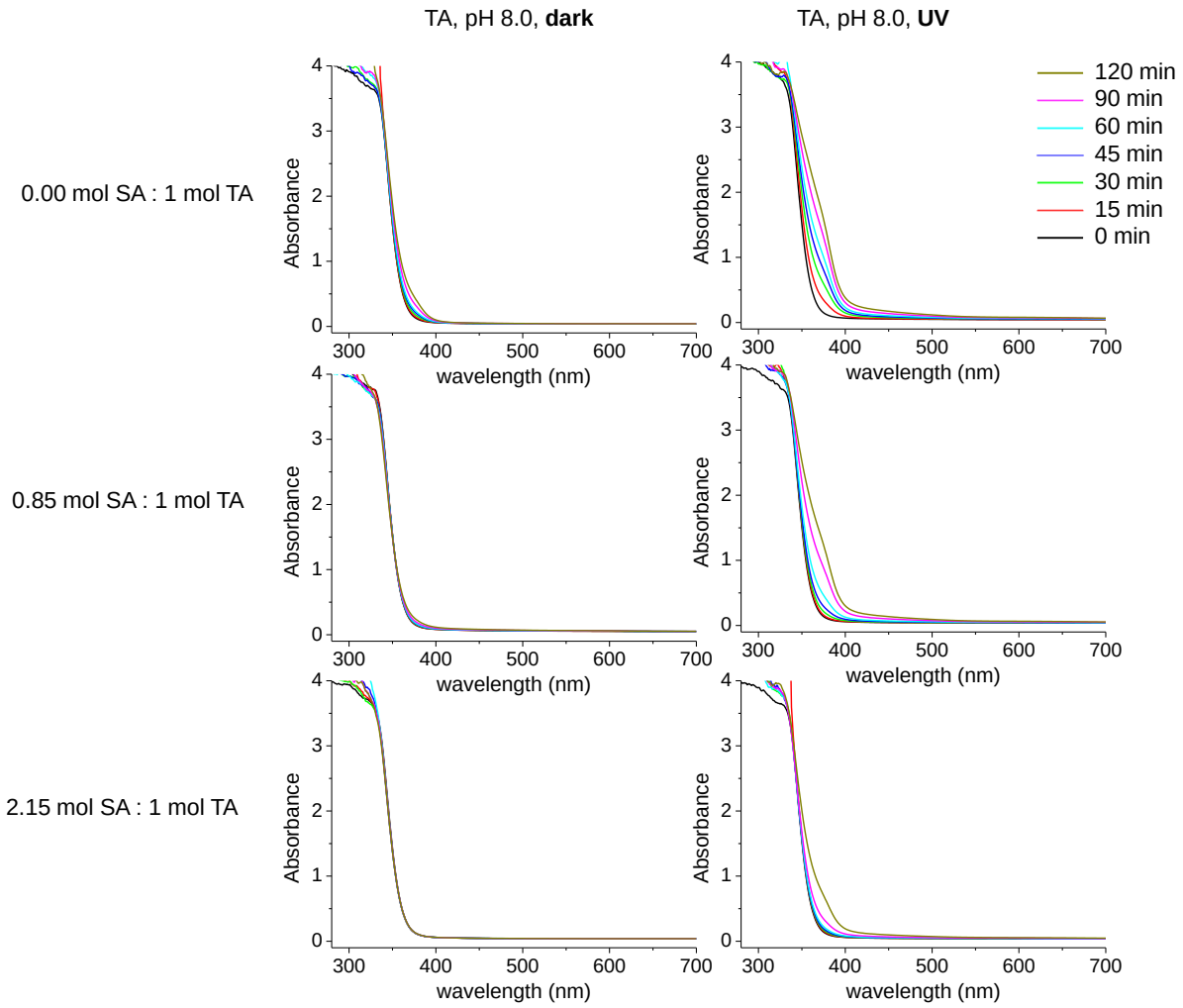

Figure S11. UV-vis spectra of TA solution (0.2 mg/mL) at phosphate buffer 5 mmol/L at pH 8.0, stored in dark environment (left) and after UV irradiation (right) containing SA measured at different time intervals.

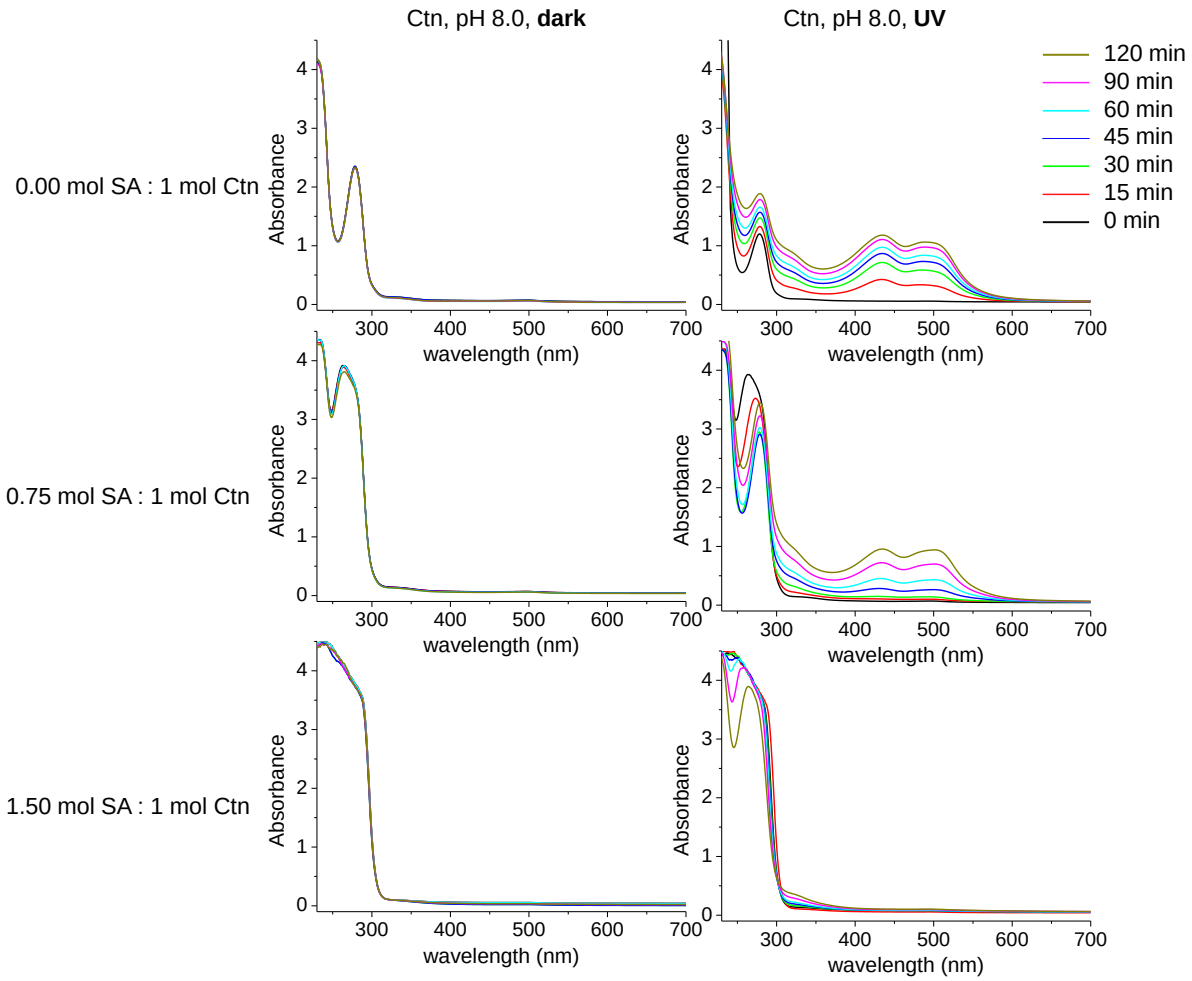

Figure S12. UV-vis spectra of Ctn solution (0.2 mg/mL) at phosphate buffer 5 mmol/L at pH 8.0, stored in dark environment (left) and after UV irradiation (right) containing SA measured at different time intervals.

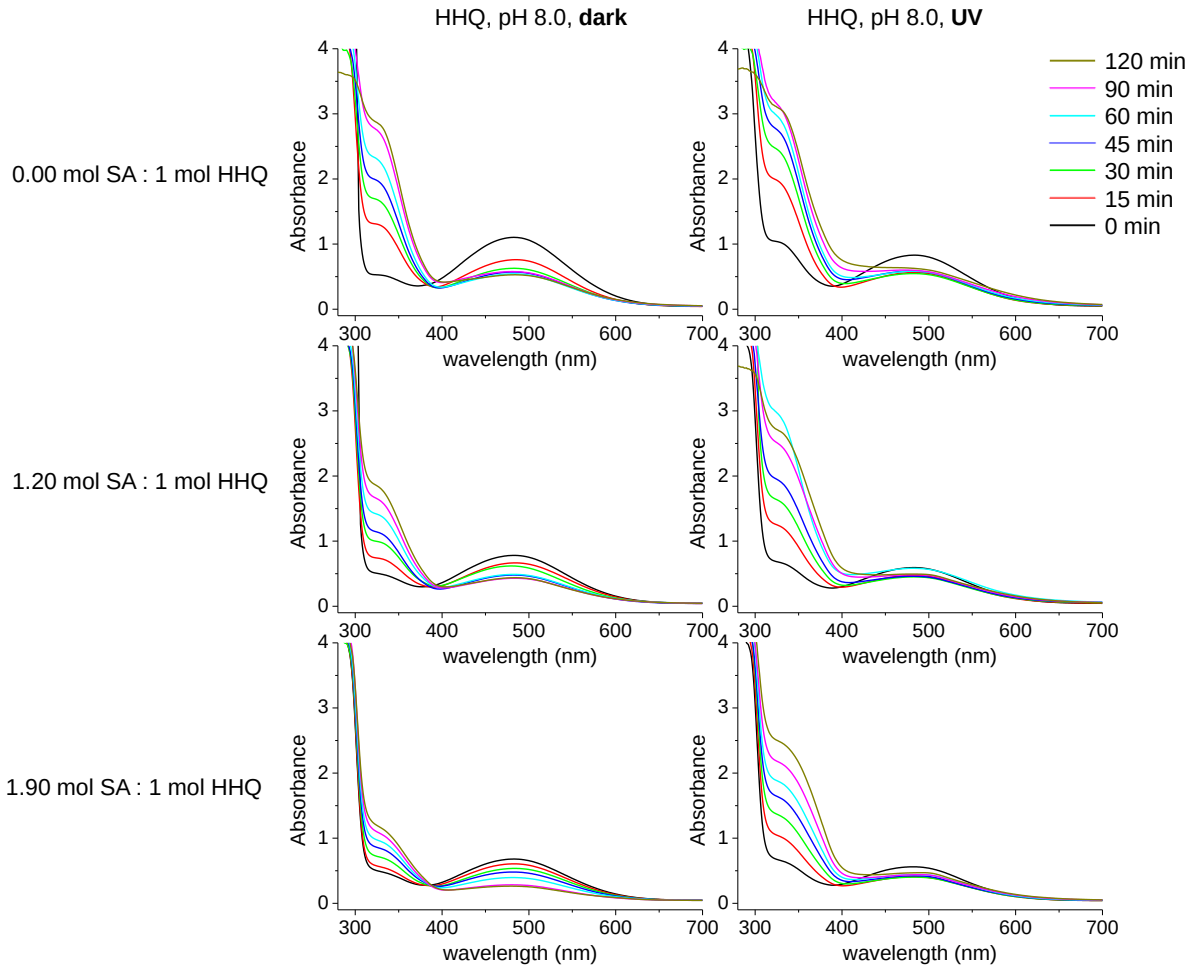

Figure S13. UV-vis spectra of HHQ solution (0.2 mg/mL) at phosphate buffer 5 mmol/L at pH 8.0, stored in dark environment (left) and after UV irradiation (right) containing SA measured at different time intervals.

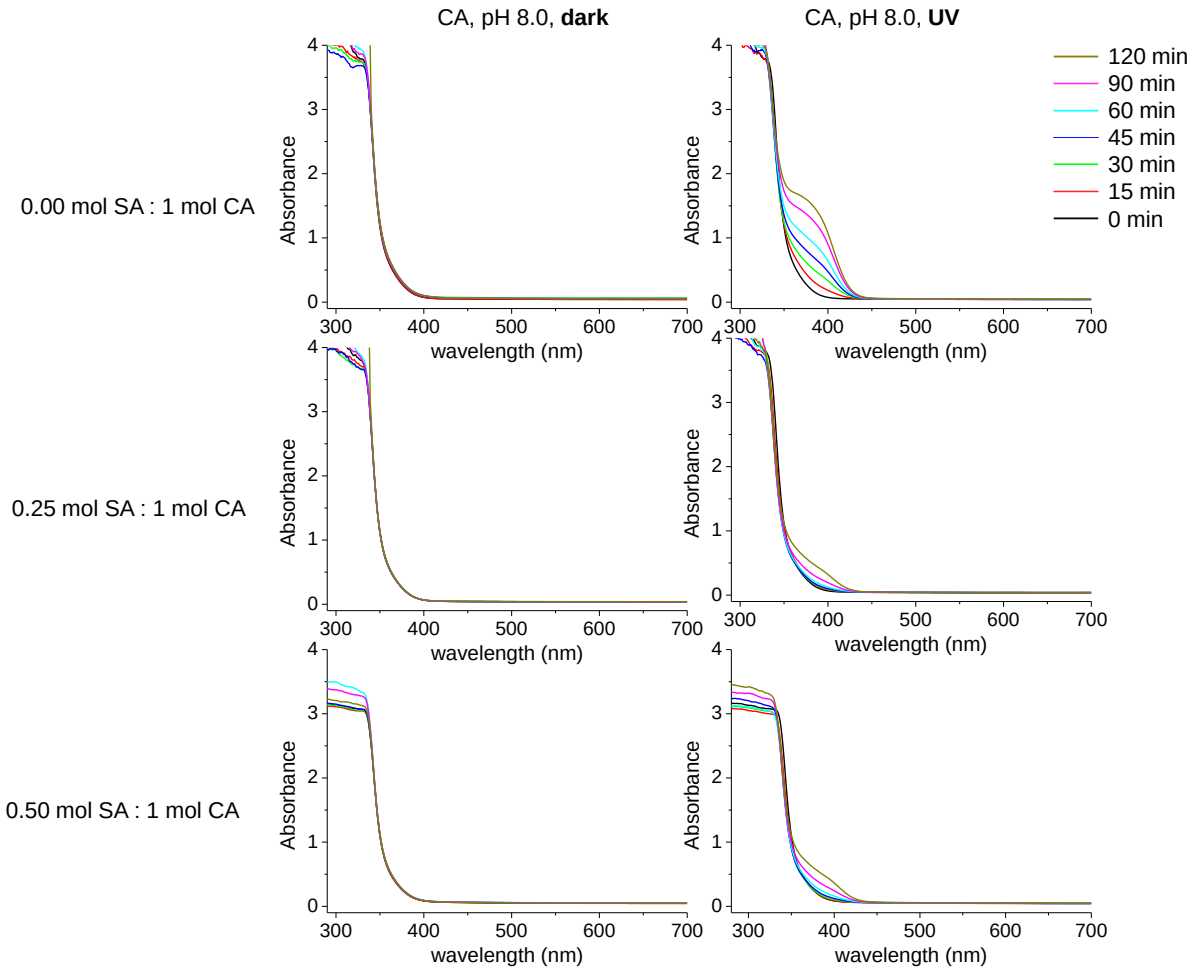

Figure S14. UV-vis spectra of CA solution (0.2 mg/mL) at phosphate buffer 5 mmol/L at pH 8.0, stored in dark environment (left) and after UV irradiation (right) containing SA measured at different time intervals.

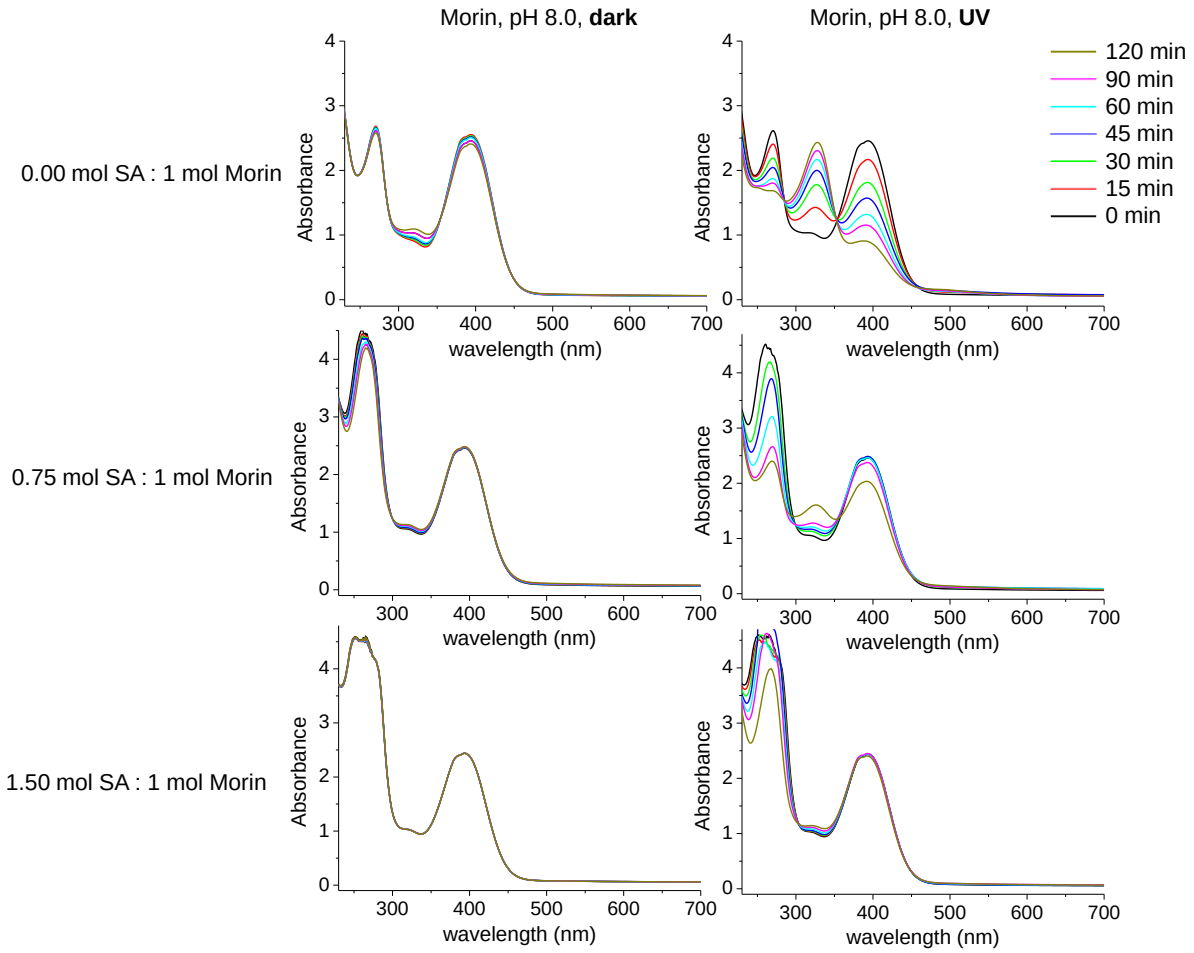

Figure S15. UV-vis spectra of morin solution (0.2 mg/mL) at phosphate buffer 5 mmol/L at pH 8.0, stored in dark environment (left) and after UV irradiation (right) containing SA measured at different time intervals.

Table S1. SA:phenol molar ratios at which oxidation of phenolic compounds is completely stopped for at least 2h

Plant phenolic compound	SA:phenol molar ratio
PG	1.20
GA	0.44
Ctl	0.60
EGCG	2.20
TA	2.15
Ctn	1.50
HHQ	1.90
CA	0.50
Morin	1.50

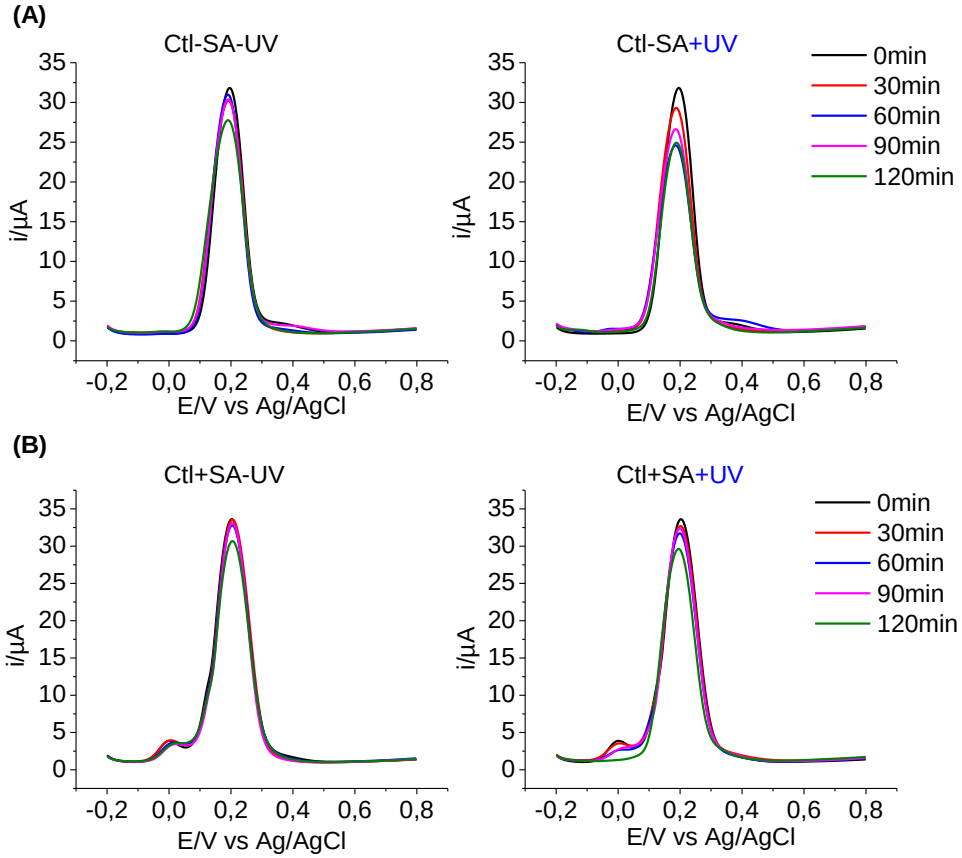

Figure S16. Differential pulse voltammetry (DPV) in phosphate buffer (5 mmol/L, pH 8.0) with KCl (0.1 mol/L) at activated glassy carbon disk electrodes for (A) Ctl solution (1.58 mmol/L of Ctl in phosphate buffer, 5 mmol/L, pH 8.0) stored in dark (left) or under UV irradiation (right) for 2h and (B) SA-Ctl solution (1.58 mmol/L of Ctl in phosphate buffer, 5 mmol/L, pH 8.0; 0.6:1, SA:Ctl molar ratio) stored in dark (left) or under UV irradiation (right) for 2h.

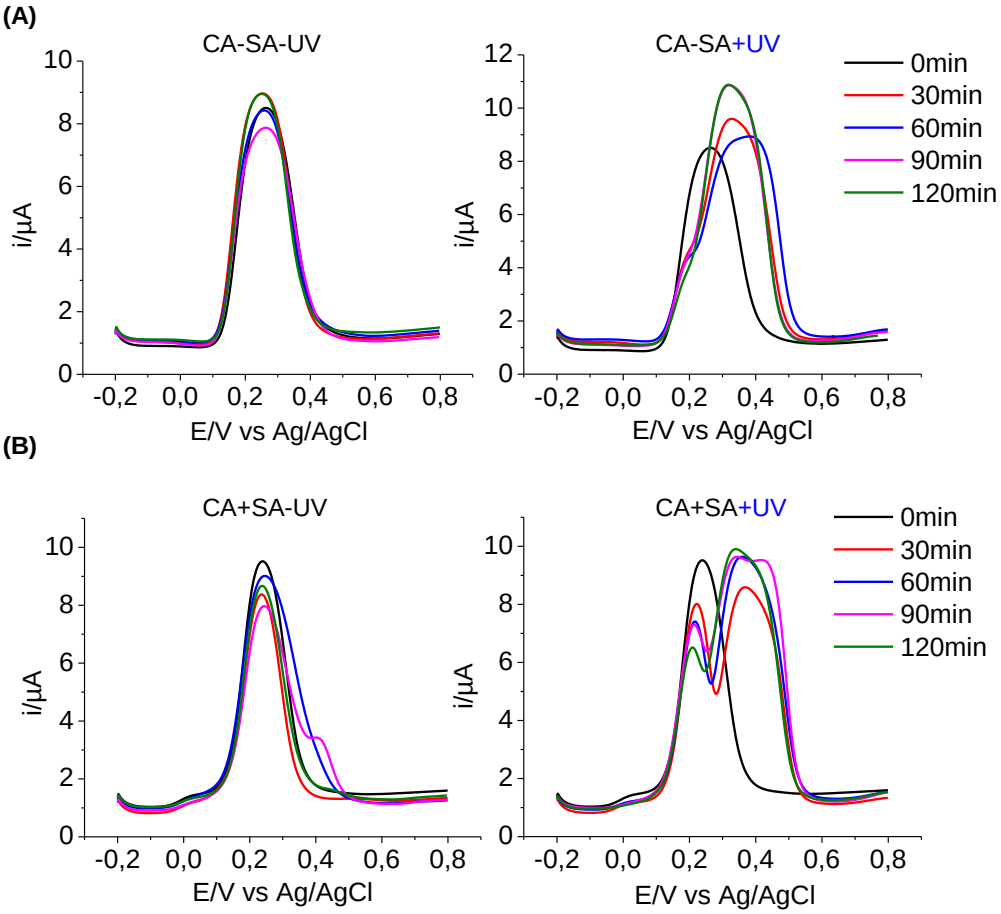

Figure S17. Differential pulse voltammetry (DPV) in phosphate buffer (5 mmol/L, pH 8.0) at activated glassy carbon disk electrodes for (A) CA solution (1.58 mmol/L CA in phosphate buffer, 5 mmol/L, pH 8.0) stored in dark (left) or under UV irradiation (right) for 2h and (B) SA-CA solution (1.58 mmol/L CA in phosphate buffer, 5 mmol/L, pH 8.0; 0.5:1, SA:CA molar ratio) stored in dark (left) or under UV irradiation (right) for 2h.

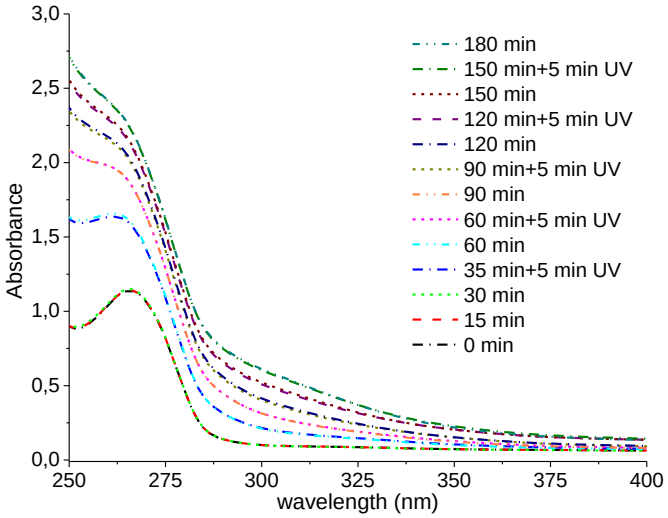

Figure S18. On-demand polymerization and of PG. UV Absorbance of the PG solution (0.2 mg/mL, phosphate buffer 5 mmol/L, pH 8.0) containing GSH with GSH:PG molar ratio of 0.8:1 at 320 nm as a function of time.

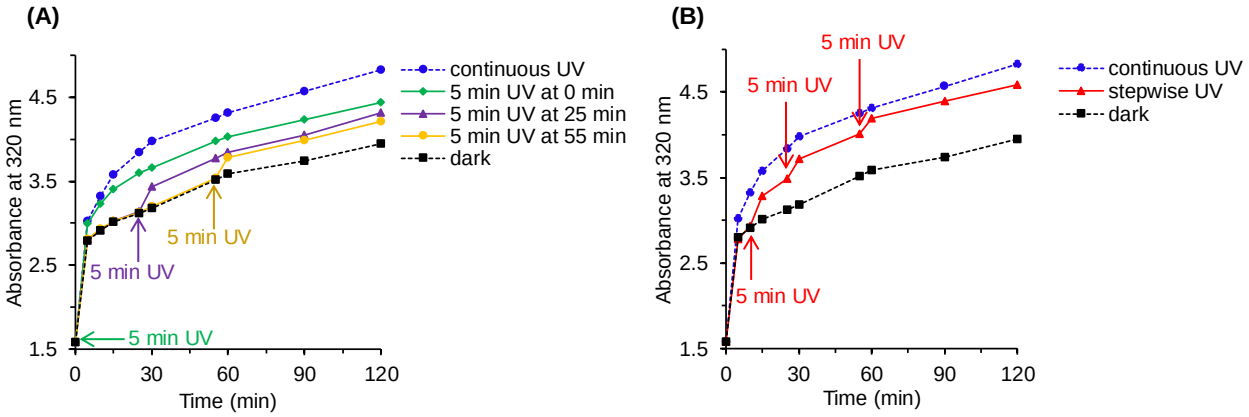

Figure S19. Timewise UV irradiation of PG solution (0.2 mg/mL, phosphate buffer 5 mmol/L, pH 8.0) in the absence of antioxidants. UV Absorbance of the PG solution at 320 nm as a function of time recorded after 5 min UV pulse at 0 min, 25 min, and 55 min (A), and after multiple 5 min UV pulse at 10 min, 25 min, and 55 min (B).

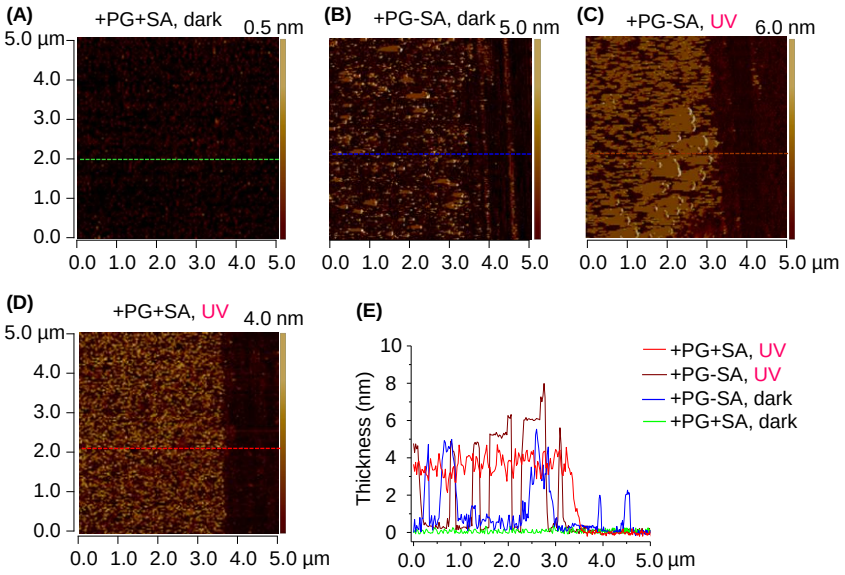

Figure S20. AFM on silicon surfaces exposed to PG solution at pH 8.0 (5 mmol/L) with SA in dark (A), without SA in dark (B), without SA under UV irradiation (C), and with SA under UV irradiation (D) for 30 min. The obtained images indicate a more homogeneous phenolic layer is deposited on the surface in the presence of SA after 30 min UV irradiation at pH 8.0. Surface topographies measured along the dashed line are shown in the graph (E).

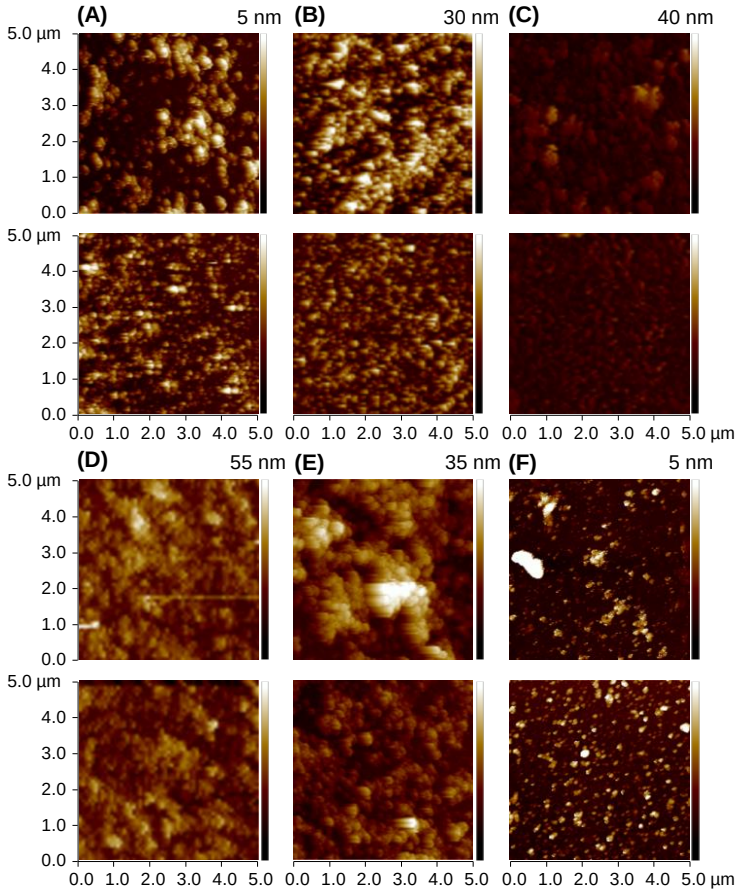

Figure S21. AFM images of phenolic layer made on silicon surfaces exposed to exposed to phenolic solutions at pH 8.0 without Antioxidant (top image) stored overnight in dark environment, and phenolic solutions containing SA irradiated with UV light for 30 min (bottom image). (A) Ctl, R_q(top, bottom)=(4.11 nm, 3.03 nm). (B) EGCG, R_q(top, bottom)=(20.1 nm, 12.5 nm). (C) TA, R_q(top, bottom)=(25.2 nm, 11.4 nm). (D) Ctn, R_q(top, bottom)=(38.3 nm, 36.5 nm). (E) HHQ, R_q(top, bottom)=(26.2 nm, 15.9 nm). (F) Morin, R_q(top, bottom)=(3.72 nm, 2.83 nm).

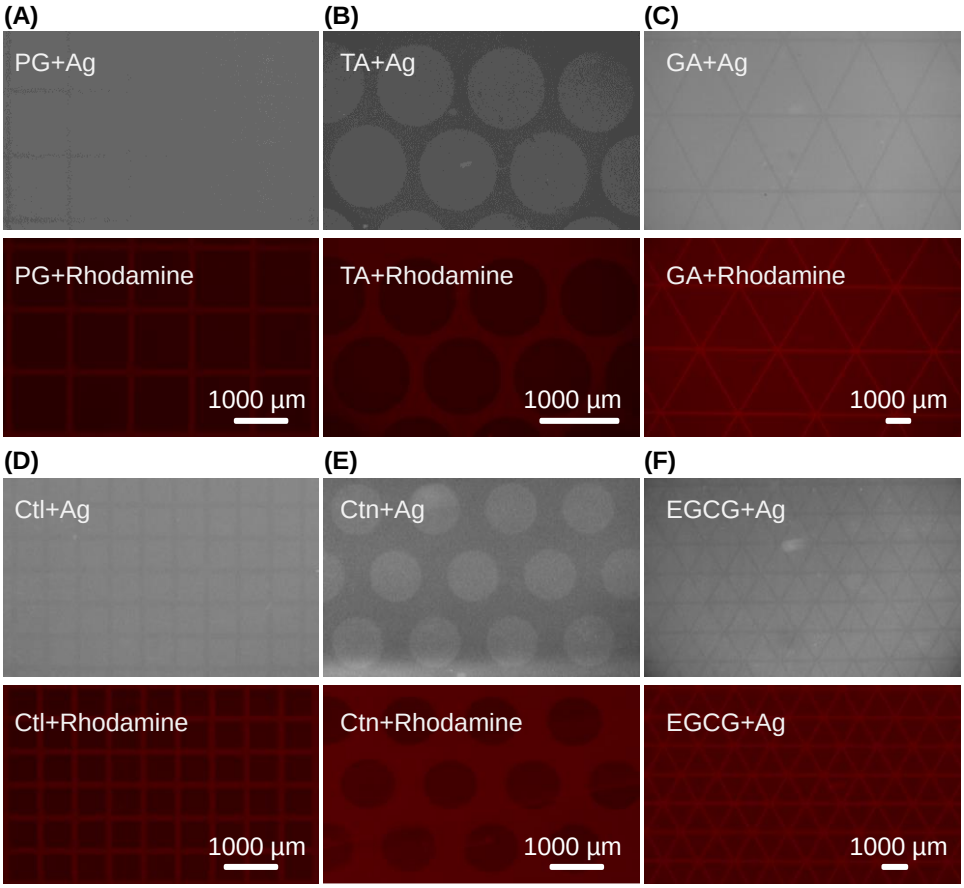

Figure S22. Photopatterning of different plant phenolic compounds in the presence of SA in phosphate buffer (5 mmol/L, pH 8.0). (A-F) Micropatterns of PG, TA, GA, Ctl, Ctn, and EGCG on poly(HEMA-EDMA) surfaces by UV irradiating of the phenolic precursor solution containing SA through a photomask for 10 min. The micropatterns were post modified by silver or Rhodamine. The images were obtained by bright field (top) and fluorescence (bottom) microscopy.

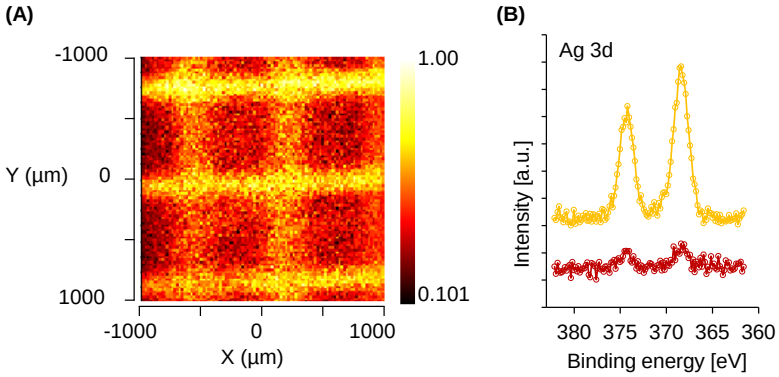

Figure S23. XPS Characterization of silver deposition on the phenolic pattern. A phenolic pattern was deposited on the surface by irradiating PG solution (0.2 mg/mL, phosphate buffer 5 mmol/L, pH 8.0) containing SA with SA:PG 0.3:1 molar ratio through a photomask. The pattern was secondary modified with silver particles by immersing in silver nitrate aqueous solution overnight and subsequent washing with water and drying with N2 (A) Principal Component Analysis of all Ag 3d spectra of the area was carried out. The yellow lines show the presence of Ag whereas the dark squares prove the absence of Ag. (B) Ag 3d XP spectra measured on the line (yellow curve on top) and in the square (red curve on bottom) clearly indicates deposition of silver on the phenolic pattern.

Secondary modification of a phenolic pattern based on PG with silver particles was analyzed by XPS. Since the poly(HEMA-EDMA) surface contains a lot of C-O species, no clear difference in the C 1s spectrum can be observed after coating with different phenolic compounds. The introduction of silver in the coated regions allows the further detection of the doublet Ag 3d and its mapping on a defined area of a structured sample consisting of lines (polyphenolic coating) and squares (non-coated). The obtained spectra were analyzed with Principal Component Analysis (Figure S20A) in order to improve the differentiation of the different regions. The spin-orbit doublet with Ag $3d_{5/2}$ at 368.2 eV can be clearly found on the line whereas just a noisy signal is detected in the squares (Figure S20B).

REFERENCES

(1) Nimse, S. B.; Pal, D. Free radicals, natural antioxidants, and their reaction mechanisms. *Rsc Adv.* **2015**, *5*, 27986-28006.